Available online at www.sciencedirect.com

jmr&t
Journal of Materials Research and Technology

www.jmrt.com.br

Original Article

Surface properties of AISI 4140 steel modified by pulse plasma technique

Yıldız Yaralı Özbek*

Sakarya University, Metallurgical and Materials Engineering Department, Esentepe Campus, 54187, Sakarya, Turkey

ABSTRACT

The pulse plasma process is a kind of surface modification technique. In this study, the microstructure and mechanical properties of pulse plasma-treated AISI 4140 steel were studied. Four different sample-plasma gun nozzle distances and three different pulses were chosen for the surface modification at a constant battery capacity of 800 mf. The samples were subjected to optical microscope, SEM and EDS analyses, microhardness testing and X-ray diffraction (XRD) analysis. The columnar and fine grained structures were formed in modified layer. New and hard phases were formed on the modified layer. Hence, the hardness increased five times after pulse plasma treatment. The amount of wear for all specimens was evaluated by using the reciprocating wear (linear wear test machine) test with a 0.15 m/s constant sliding speed under 5, 7, and 9 N loads along a 200 m sliding distance. A WC ball (with 6 mm diameter) was used in this test. The friction coefficient and wear rate were changed in accordance with the applied load. The friction coefficient values decreased and the wear resistance increased in the surface-modified specimens compared to the non-modified ones. The wear rate and the friction coefficient were changed with the wear debris and load. The debris was increased by the resistance to wear of surface. The worn surfaces of the specimens were studied by using atomic force microscopy (AFM), scanning electron microscopy (SEM) and electron dispersive spectroscopy (EDS). The abrasive wear was shown on worn surface.

1. Introduction

The microstructure of tool steels and their surface properties can be modified with different surface treatment processes by pulsed laser, ion or plasma beams [1–6]. As one of the surface modification techniques, the pulse plasma process is widely used to improve the surface properties of tool steels. [4–7].

The pulse plasma system consists of; the elasto-plastic deformation, impact by sound and the pulsed magnetic field, heat, electric-pulse treatment, deformation of the metals and alloys during the operation. A jet having energy density is formed via the detonation combustion of fuel gas mixtures. Superposition of an electromagnetic field onto a detonation wave transforms the latter into a plasma pulse due to the presence of extra energy present [4]. The surface layer of the target

* Corresponding author.
  E-mail: yyarali@sakarya.edu.tr
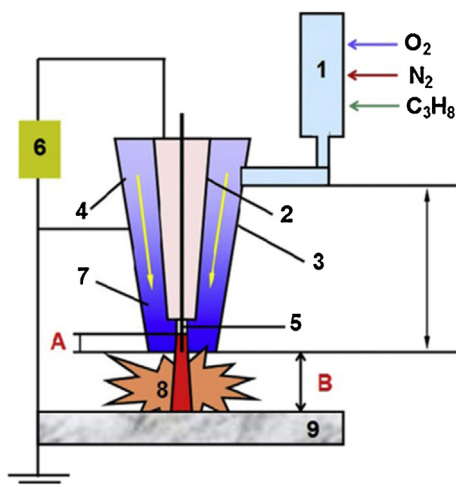
Fig. 1 – Schematic presentation of the pulsed-plasma modification system: 1-detonation chamber, 2-central electrode, anode, 3-conical electrode, cathode, 4-interelectrode gap, 5-consumable electrode, 6-power supply, 7-gap between the electrodes, 8-pulsed plasma forming, 9-work surface.

Table 1 – Chemical composition of 4140 steel used for pulse plasma surface modification.

%W	C	Si	Mn	P	S	Cr	Mo
AISI 4140	0.40	0.30	0.70	0.035	0.035	0.98	0.27

Table 2 – Sample codes and the pulse plasma parameters of the specimens.

Sample no	Nozzle-sample spacing (mm)	Number of pulse
1	70	15
2	70	10
3	70	5
4	80	15
5	80	10
6	80	5
7	60	15
8	60	10
9	60	5
10	50	15
11	50	10
12	50	5

expose to a rapid melt and solidification with heating and cooling rates typically in the range of 10^7–10^{10} K/s. After the pulse plasma process, the surface layer can have high anti-friction properties and wear resistance. The pulse plasma has no size limitation or residual stress problems, and thus, it is a suitable surface modification technique to treat complex-shaped industrial components [1–4,6]. Compared to laser treatment, electron beam treatment and conventional ion implantation, Pulse plasma treatment has high energy conversion and processing efficiency and facile processing [6–8].

In this work, the substrate was chosen as AISI 4140. AISI 4140 steel, which is easily obtainable and extensively used for industrial surface modification applications, was studied to determine the effects of pulse plasma treatment parameters on the structure. The chromium–molybdenum alloy steels are known to be widely used in the structural, automotive and gas industries due to their superior hardenability and high strength [7,8]. In addition, the effects of the pulse plasma parameters on the reciprocating sliding wear properties and the related wear mechanisms were investigated.

2. Experimental procedure

2.1. Pulse plasma treatment

The pulse plasma system is shown in Fig. 1. The plasmatron consists of a detonation chamber where the fuel gas mixture is occured and its detonation combustion is initiated, a central electrode-anode, a conical electrode-cathode, inter-electrode gap (4), a consumable electrode (5) and a power supply (6).

The cyclic thermal effect with a frequency of 3–5 Hz leads periodic heating of the surface up to a melting point, which alters the phase state of the metal layer and accelerates the transfer of alloying elements. Multiple heating and cooling of

the surface layer with high temperature gradients cause to periodic changes in stresses and strains in this layer, which leads to substantial changes in the structural state of a metal alloy. Plasma-detonation treatment is participated by a pulsed mechanical pressure of the high-velocity plasma jet. The energy (up to 4 kJ) of free gas-dynamic shocks is determined by mass and velocity of the plasma jet. Mechanical effect is considered to be an efficient means on the acceleration of chemical and mass-exchange processes occurring in a solid body. It activates oscillation processes in a metal alloy, excites long-wave acoustic phonons, thus accelerating cooling and crystallisation, and intensifies mass transfer of alloying elements in the heated layer [1].

The work piece surfaces of the samples were subjected to detonation process accompanied under a plasma atmosphere containing alloying elements dissolved from the metal electrode rod in interaction with the constituents of propane and nitrogen gases used for the process. The tungsten was chosen as consumable electrode in this work. This process provided the workpiece surfaces with alloying of plasma components and hardening of surfaces [1,4,7,8].

Because it is cost effective and commonly used in industrial applications, AISI 4140 steel was selected as the substrate material. The chemical composition of the AISI 4140 steel was given in Table 1. The diameter of the cylindrical samples was 22 mm, and their thickness was 10 mm. They were machined by a CNC lathe. The machined samples were not subjected to any treatment prior to the pulse plasma. The process parameters that were applied to the machined samples were presented in Table 2 with their sample codes.

2.2. Surface characterization

After the pulse plasma surface modification, the cylindrical specimens were cut in to cross-sections to measure the case depth. The specimens were grinded by 120, 240, 320, 400, 600, 800, 1000, 2400 and 4000 mesh emery papers. Then, the samples were polished with 3 μm diamond paste and etched by
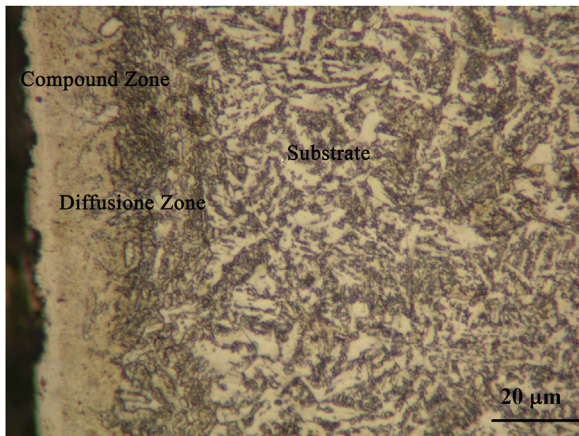
Fig. 2 – Micrograph cross-section of modified AISI 4140 steel samples (distance 40 mm, 10 pulse).

using 3 wt. % nital solution; then the microstructures were observed by means of an optical microscope, SEM and EDS (JEOL-JSM 6060 L V). The structures of pulse plasma-treated samples were investigated by X-ray diffraction (XRD) by a Rigaku D/MAX/2200/PC model device with Cu-K$_\alpha$ radiation ($\lambda = 0.154056$ nm).

The cross-sectional hardness values of the specimens were measured at a spacing of 10 μm from the modified surface at 5 g loads for a dwell time of 15 s (Leica VMHT device). Three sets of cross-sectional microhardness measurements were carried out for each sample.

2.3. Wear tests

Wear and friction tests were performed in a linear wear test machine named CSM tribometer. The tests were carried out at ambient temperature (28 °C ± 3 °C) under a controlled humidity that was between 40 and 50 % under dry sliding conditions. The sliding distance (way) is 12 mm on wear surface. The reciprocating sliding mode was calculated with a 0.15 m/s constant sliding speed under 5, 7 and 9 N loads in a 200 m sliding distance. Each of the tests was repeated at least three times to ensure the accuracy of the obtained wear and friction values A spherical counter-part was oscillating under the load against the modified steel sample. A WC ball with a 6 mm diameter was utilized as the counter-part. The friction force was continuously recorded by the sensors at the test block so that the coefficient of friction could be calculated with respect to normal force. The results shown here were selected from numerous tests performed at different samples. The friction coefficient and the wear rate varied as a function of load. The system enables measuring friction coefficient and time dependent depth profiles by using sensitive transducers. The depth transducer was located vertically on top of the sample.

After the wear test, the worn surfaces were characterized by SEM, EDS and AFM analysis. The calculations of the wear rate were performed by using a Perthometer MAHR surface roughness apparatus after the wear test. The amount of wear on the surface after each test was calculated by measuring the wear width, depth and the amount of surface roughness by using a surface profilometer and low magnification optical micrographs.
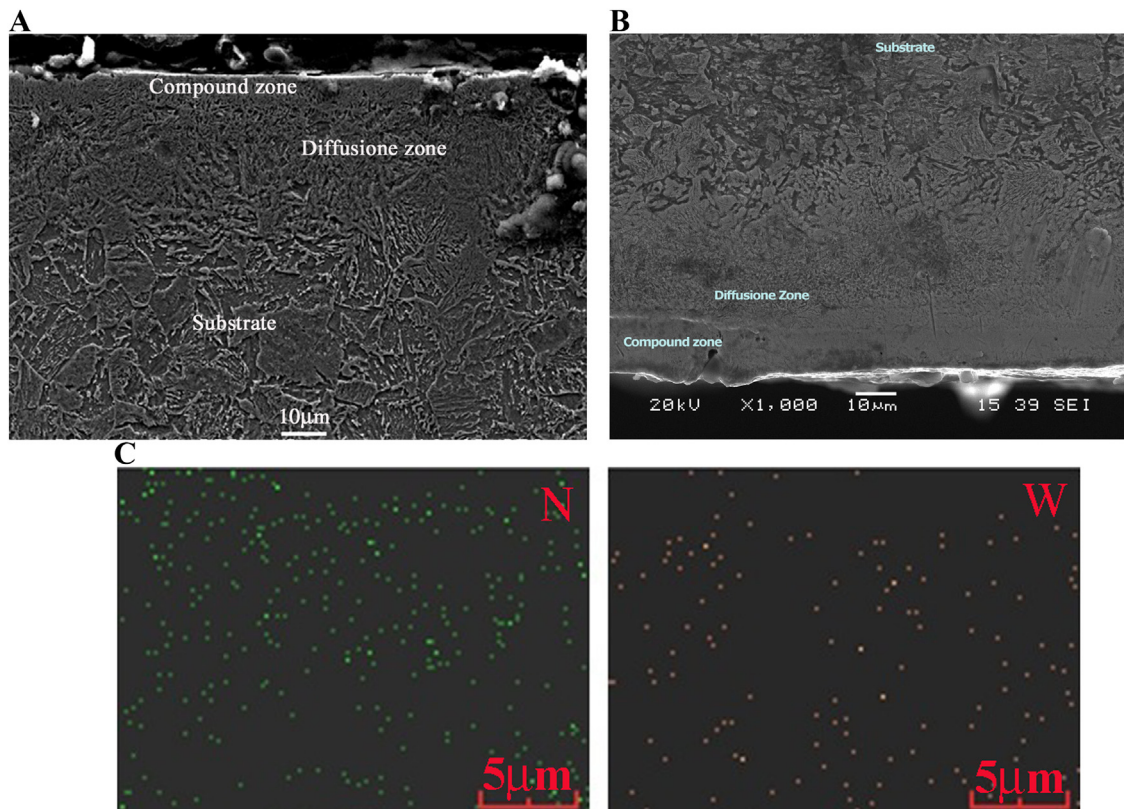
Fig. 3 – SEM micrograph of (a) sample 11 (50 mm–10 pulse), (b) sample 7 (60 mm–15 pulse).
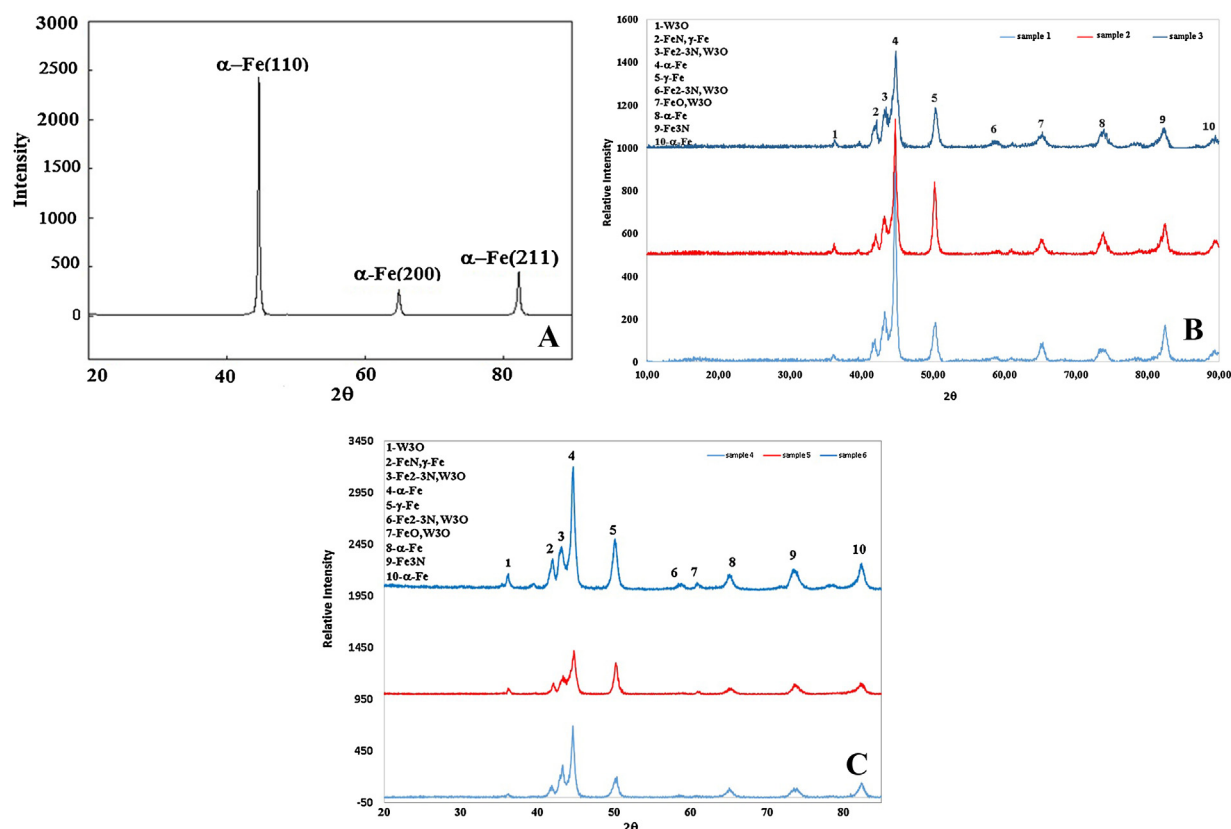
Fig. 4 – XRD results of (a) untreated sample, (b) sample 1, sample 2 and sample 3 (70 mm distance, 15-10-5 pulse number), (c) sample 4, sample 5 and sample 6 (80 mm distance, 15-10-5 pulse number).

3. Results and discussions

Fig. 2 shows the optical micrograph of modified sample. As expected, for classical surface modification treatments, a surface layer was composed of an external compound layer with an underlying diffusion layer [9–13].

The compound layer, the diffusion layer and the substrate were easily observed due to the contrast in colour. Nitrogen that was diffused into the steel surface was combined with an alloying element along the electrode to form fine dispersed nitrides. As a result, a thin iron nitride layer, which composes of nitride phases that is mentioned to the white layer due to the lack of etchant, was produced on the surface [16]. There were high concentration of nitrogen ions and the presence of weighty non- ionized nitrogen molecules (compound layer) [11]. The compound layer has a porous structure. These findings are similar to the experimental results reported by Sirin et al. [10]. Stahli and Sturzenegger investigated the formation of a thin modified layer of a new structure and same results were observed [12].

Depending on the nitrogen concentration in the gas mixture utilized during pulse plasma process, the compound layer may be constituted by ε-Fe2–3 N or γFe-Fe4N phases or a mixture of both.

Fig. 3(a and b) shows SEM micrograph of sample 11 (50 mm–10 pulse) and sample 7 (60 mm–15 pulse). In these figures, plastic deformation presents in the modified surface
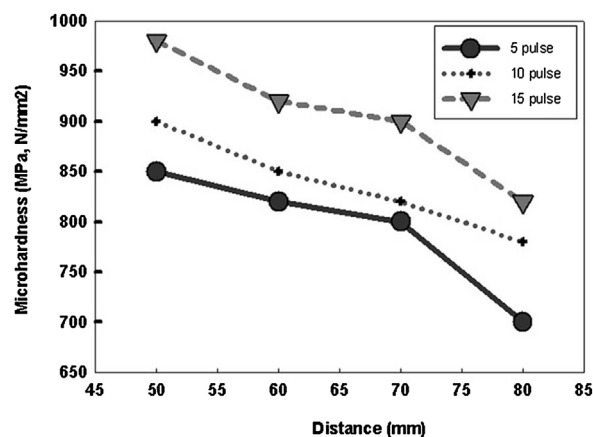

Fig. 5 – Relationship between pulse plasma parameters and microhardness.

layer, where the microstructural morphology differs from the matrix. Existence of a very fine microstructure was associated with the plastic deformation, which was believed to occur because of the repeated heating and cooling due to the increasing number of pulses. The deformation of metallic materials can enhance the nitrogen diffusion into iron, leading to a decreased grain size and dislocation density [16].

The thickness of the modified layers was changed as a function of the different process parameters. When the number
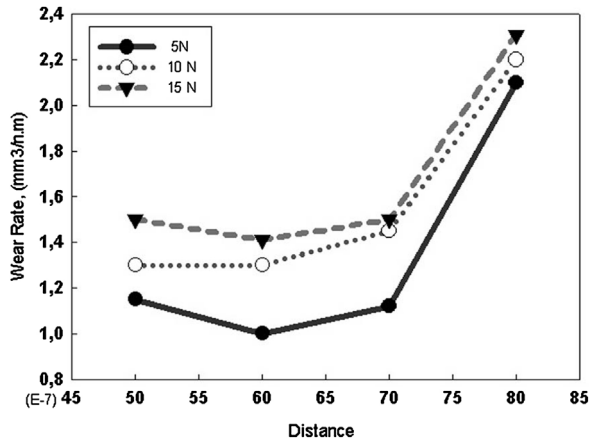
Fig. 6 – The relationship between the wear rate and applied load for modified samples for 5 pulse.
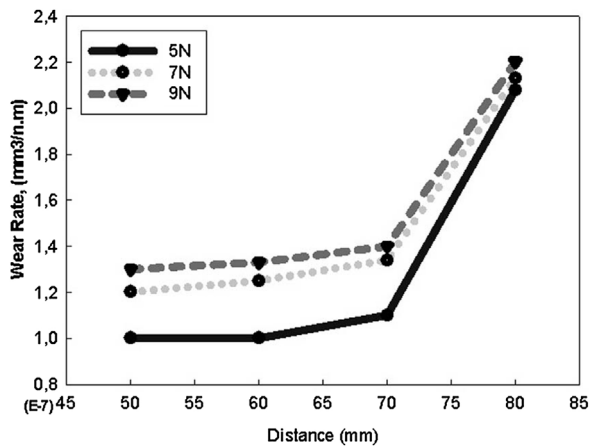

Fig. 7 – The relationship between the wear rate and applied load for modified samples for 15 pulse.

Fig. 8 – The friction coefficient values for different load, nozzle spacing and pulse numbers.

of pulses was increased, the compound and diffusion layer thicknesses were also increased shown in Fig. 3(a and b) [11]. This effect is due to the high temperature of the surface during the plasma treatment which results in the melting surface layer and the subsequent liquid phase mixing of the ionized gases, which were deposited earlier, with the substrate material [12,15]. Thus, an increase in the pulse number results in a deeper penetration of tungsten and nitrogen into the bulk, and tungsten and nitrogen-rich layers are produced on the steel surface. Yang Li et al. [9] also reported the same findings for 4140 steel.

Additionally, the nozzle-sample spacing is another important parameter. Increasing the nozzle distance resulted in a decrease in thickness of the modification layer due to the projectile effect of the plasma. Another reason for this decrease is that the ionized gases that were exhausted from the nozzle could not reach the surface of the specimen clearly and homogeneously. When the nozzle-sample distance decreases, the surface is overheated. The fused areas can be seen on the surface in this case. These results are in agreement with the literature as [10,14] Tyurin and friends reported the same results [8].
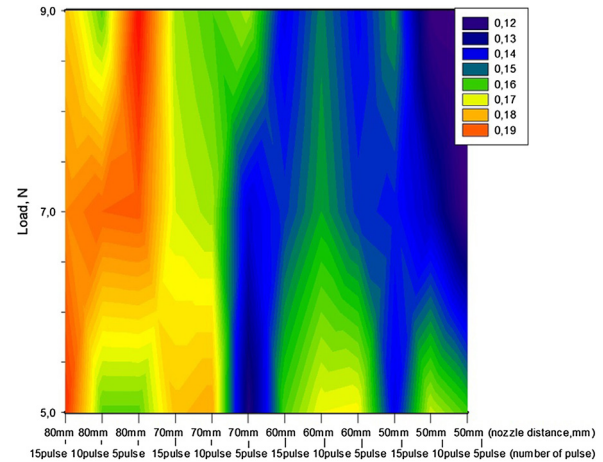
This process was also applied to M2 steel surface [20]. The M2 steel (high speed steel) is high alloy steel. However, the same morphology was observed in both steels [20]. These works show that, the pulse plasma process can be applied to the steels whose carbon content is higher than 0.4 wt. % C. High amounts of alloying elements in steel are not necessary for this process.

Fig. 4 shows the X-ray diffraction profiles of the untreated sample and the samples modified by the pulse plasma. Samples 1, 2 and 3 were treated in 70 mm spacing with 15, 10, 5 pulses, respectively; samples 4, 5 and 6 were treated in 80 mm spacing with 15, 10, 5 pulses, respectively. The samples contained strong diffraction peaks for the α-Fe phase, as well as weak diffraction peaks for γ-Fe, Fe_2-$_3$N (hcp), W_3O and FeN [16,20]. The nitride and tungsten-rich phases can be formed during short pulse heating, the interaction of the phases have introduced impurities, and further rapid cooling [9–11]. Additionally, the intensity of diffraction peaks decreased compared to the untreated specimen, which suggests that the grains of the pulse plasma-treated specimen were refined and the mean lattice microstrain was increased. The amount of tungsten oxide phase increases with decreasing the nozzle-sample spacing as observed in sample 1. Li et al. suggested that the Fe_2-$_3$N and FeN nitride phases increased due to the increasing pulse number [13].

The XRD pattern of the treated specimen shows that the full width at half maximum (FWHM) of the diffraction peak was broadened. It has been well known that the FWHM broadening occurs as a result of decreased grain size [21–23]. The residual stress occurs after rapid pulse-treatment. The compressive residual stress on the surface lead to a broadening of the diffraction peaks [21].

Fig. 5 displays the microhardness values of the samples as a function of different parameters. The highest surface microhardness value of the modified AISI 4140 steel was measured as 950 $HV_{0.05}$ at a 15 cycle pulse and 50 mm nozzle spacing, whereas the lowest microhardness value was measured as 700 $HV_{0.05}$ at 5-cycle pulse and 80 mm nozzle spacing. The hardness increased 5 times with respect to original, untreated base metal that was measured as 180 HV.
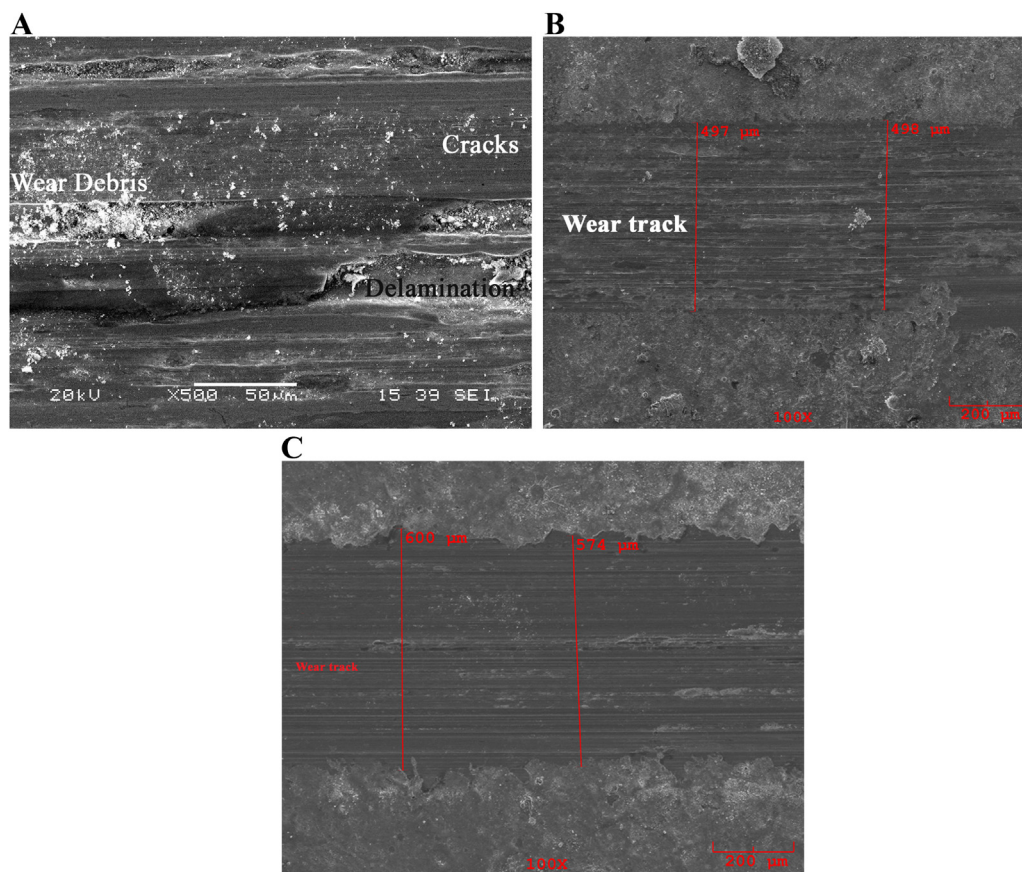
Fig. 9 – SEM analyses of samples after wear testing (a), untreatment sample, (b) wear track of sample 2 for 5 N, (c) sample 2 for 7N.

The hardness gradually decreases due to the alloy concentration near the core, resulting in a diffused case–core interface. The fast cooling and solidification of surface melting material could produce very fine microstructure. The surface layer consisted of nano-crystalline grains and a plastic layer that was severely deformed, which is composed of sub-grains with many defects, such as dislocations and grain boundaries that can be formed in the pulse plasma method. The ultra-fine grains are one of the reasons for surface hardening. The microstructure of modified surface will become finer with increasing number of pulses [11].

The relationship between a material's micro-hardness and its grain size can be explained by the Hall–Petch formula;

$$\sigma y = \sigma_0 + ky/\sqrt{d}$$

Where σ_y is the yield strength of material which can usually be replaced by micro-hardness (HV), σ_0 is the lattice friction resistance, k_y is a constant, and d is the average grain diameter. According to this equation, the micro-hardness of a material is inversely proportional to its average grain size. In addition, the nanostructured surface layer of the AISI 4140 steel significantly promotes the diffusion of gases when many pulses are used, resulting in the formation of new hard phases [24]. We can safely propose that the hard phases and new structure improved the surface hardness [25–27].

The pulse plasma process can be applied to different steel groups [28]. Not only the 4140 steel but also M2 steel hardness values were increased after the pulse plasma treatment. The hardness values of high speed steel (i.e.M2) was increased 4 times [20]. This property is very important to steel industries.

During the modification process, the rapid heating and cooling generates small grains resulting in better wear resistance [13,14]. The hard compound layer could significantly increase the wear resistance of the plasma-modified 4140 steel compared to the untreated zone [28–30]. The cracks are always initiated from the contact surfaces for both untreated and pulse-plasma treated samples. The occurrence of compound layer affects the crack initiation and the columnar structure occurred in diffusion zone retards the crack the propagation on surface [13]. Therefore, the compound layer on the surface should have a significant influence on the surface wear behavior. In traditional nitriding process, the compound layer can be brittle. In pulse plasma treatment, the surface becomes much more ductile than traditionally nitrided surface [13], due to the sputtering effect during the pulse plasma process. The compound layer has a certain degree of ductility despite its high hardness. This will bring additional benefits to the modified compound layer with respect to wear protection. However, Gualtieri et al. used the Hall–Petch equation [19], and they found that the relationship between the grain size reduction and hardness increment obeys the Hall–Petch
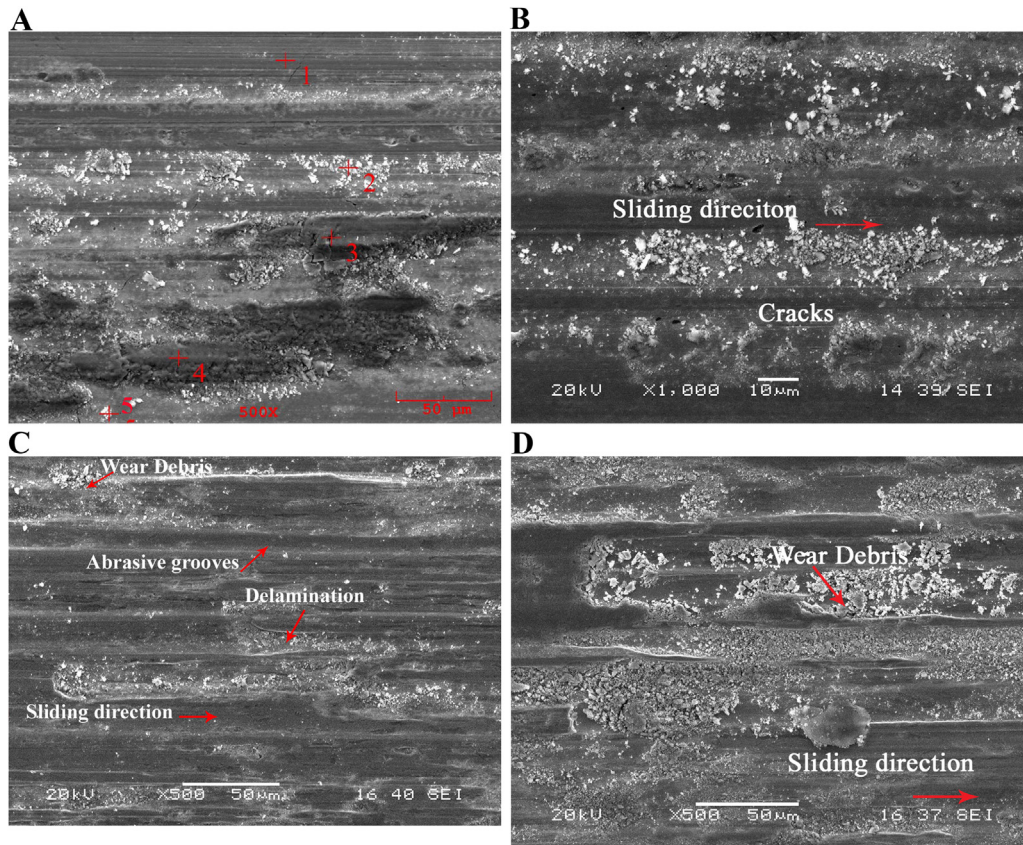
Fig. 10 – SEM and EDS results of after wear test (a) sample 3 (at 5 N load), (b) sample 3 (at 9 N load), (c) sample 7 (at 5 N load), (d) sample 7 (at 9 N load).
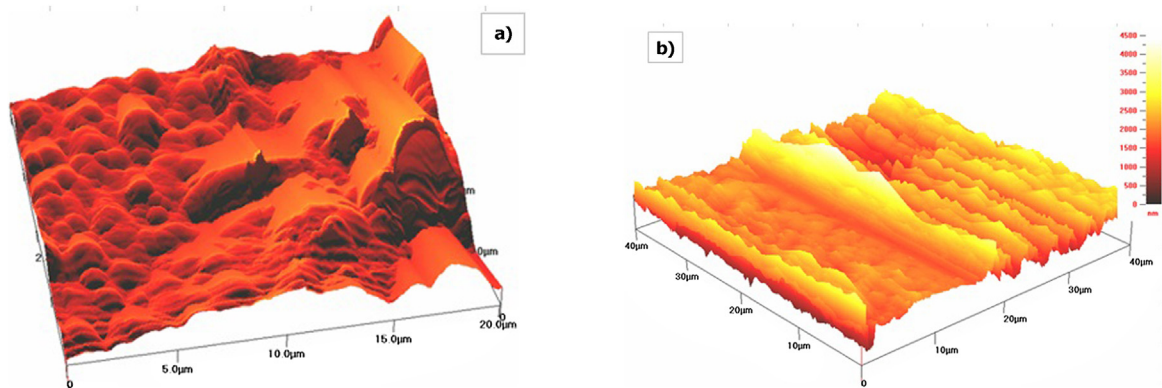
Fig. 11 – The AFM results of wear surface sample 3 for (a) 5 N load, (b) 9 N load.

behavior [13,14]. With a reduction in grain size, the dislocation activity becomes limited, preventing crack propagation and grain boundary sliding occurs (i.e Hall–Petch effect). Also, the presence of nitrogen and tungsten based phases can explain the improvement in tribological properties [24,27,28]. Because of the high nitrogen concentration in iron lattice, the significant compressive stresses occurred which has an important role in hardness increment and improves the wear resistance [6–15]. C.X. li et al. and Guan et al. indicated that the nitrogen based phases improved the wear properties of surface, sharply [12–16].

The parameters of pulse plasma affected the grain size and columnar structure. In the maintime, the increase in energy density and the number of pulses led to lower surface roughness [14]. The smaller the ratio of temperature gradient (G) to crystallization rate (R), the greater probability of fine crystalline structure formation, while a larger G/R ratio promotes the formation of columnar crystal structures. The columnar structure contributes to mechanical properties. Especially, this structure can be prevents crack propagation.

After pulse plasma treatment, the modified surface layer provided a better performance by untreatment surface. The
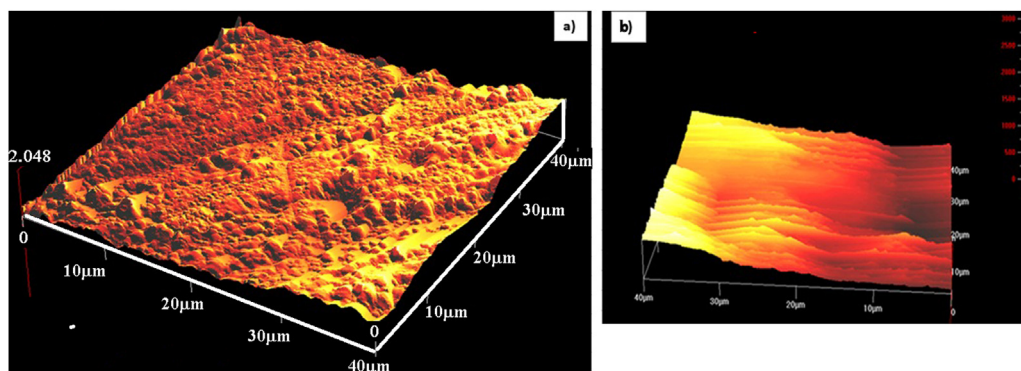
Fig. 12 – AFM results of wear surface sample 5 for (a) 5 N load, (b) 9 N load.

modified layers have been used to improve the tribological behaviour [13–15]. The effect of the nozzle distance (mm) on wear rate (mm³/n.m) for five pulses was displayed in Fig. 6. When the nozzle increases, the wear rate increases for 5 pulses. In Fig. 7, the wear rate changes with nozzle spacing when 15 pulses were used.

The wear rate decreased from 2.1×10^{-7} to 1×10^{-7} mm³/n.m after surface modification treatment. The similar ratios were calculated by Ozbek et al. [15] and Guana et al. [16]. Formation of higher amount of cracks causes fine wear debris because of small sized delamination layers formed by crack propagation, breakage and adhesion of the wear debris. The columnar structure improve the wear properties. Especially, this structure can be prevented crack propagation [17–24].

The optimum wear rate was observed in 60 mm distances. The wear rate was changed with load and pulse number. When the load was increased, the wear rate also was increased [15]. The largest wear rates were obtained under 9 N loads for all samples. The wear resistance of the modified surface increased when the number of pulses was increased. The compound layers were quite easy to be brittle after pulse plasma process. One possible solution was to enhance the number of pulses on the surface. When the number of pulses increased the wear properties of surface was improved due to high energy and alloy elements (nitride and tungsten) [10,23,25].

There fast heating and melting procedures, where the dissolution of precipitation hardening particles and interdiffusion with the encircled material will be greatly promoted. The local concentration of alloying elements can be destroyed effectively in the modification layer. Due to the short duration of pulse plasma effect of modification layer, the high-temperature surface layer undergoes superfast solidification and cooling processes. Thus, the homogenous distribution and super-saturated dissolution of alloying elements can be retained along with the formation of remelted layer oriented preferentially along direction.

With the increasing pulses the microstructure in depth of several micrometers was refined [26]. In the process of cooling, the rate of temperature change can be reached to 10^8 K/s. On one hand, this kind of extreme processing promoted precipitation of a great number of small size grain and amorphous nitride alloys [12–17] with high brittleness there was the thermal stress concentrated on modified surface. These factors were affected the wear properties. The wear properties were improved the surface properties. The pulse number was positively affected [18–20].

The coefficients of friction obtained from the wear tests for the samples under 5, 7 and 9 N were shown in Fig. 8. The friction coefficient of the untreated sample was 0.49. The coefficient of friction for the untreated sample kept increasing during the first 2−3 h and then became relatively stable at a high value. However, the friction coefficients of the modified samples only changed merely between 0.12 and 0.19. The distance affected the friction coefficient. As shown in Fig. 8, there is primarily a separate low friction coefficient window, which began at the 70 mm nozzle distance and extended to the 50 mm distance. As decreasing the nozzle distance to 50 mm resulted in an increased hardness and an increased wear resistance, the shear forces decreased and caused to low friction coefficient. One interesting result is that for the 70 mm nozzle distance under all of the applied load conditions, the friction coefficient is low.

Despite of the increased hardness for the 50 mm nozzle distance, the friction coefficient only slightly increased under low load (5 N) conditions. This is believed to be related to the wear mechanisms and the microcrack formation, and the related abrasive mechanism is responsible for the higher friction coefficient. Under the increased load conditions, the surface temperature rises and leads to more oxidation, which is beneficial in decreasing the friction coefficient.

Qualitative assessment of the wear scars was carried out using SEM. Fig. 12 shows a plan view secondary-electron (SE) micrograph. The analysis has shown the presence of the compound layer because of its compact and closely packed hexagonal structure and higher nitrogen content. The presence of a compound layer that has very good friction characteristics produced even lower friction coefficients. This result is in agreement with Fattah's study [30]. The compound layer provides the tribological characteristics, while the diffusion zone determines the strength of the modified layer. The Fig. 9(a) shows the worn surface of untreated sample. The worn surfaces exhibited a seizure of the wear debris on the sliding surface and the subsequent plastic deformation hardening, as evidenced by the micro-cracks on the surface. The abrasive wear occurred on the worn surfaces and was associated with various grooves. Thus, micro-cutting is the main wear mechanism in these samples [25].

It is also possible to serve the formation of fine wear particles, in the shape of platelets that developed in the surface of the diffusion layer. The repeated loading action by the harder asperities and/or wear debris on the softer surface induces plastic deformation, which increases with the progress of wear test. This behaviour can be explained by the complete or almost complete destruction of the superficial modified layer.

In addition to these free particles acting as a third body, there are also hard asperities on the counter-body that cause abrasion between the two bodies. It is necessary to consider that the type and configuration used in these tests, that is, the reciprocating and sphere-plane, contribute to maintain the wear debris inside the system due to the bidirectional movement and inexistence of centrifugal forces. In this type of test, the free wear debris is transported forward sand backwards, and being eliminated from the system in the perpendicular direction of the sample movement.

The wear tracks of sample 2 were shown in Fig. 9(b and c). The wear track width is 497 µm under 5 N load, while average is 580 µm under 7 N loads. The width of wear track increases with increasing wear load. During the initial period of sliding, the compound layer with a high stress fractured and then transformed the abrasive particles. After removal of the compound layer, the wear track exhibited plastic deformation and deep grooves. The widespreading wear mechanism combines the adhesive wear and abrasiveness, which was found for all of the pulse plasma-treated specimens. However, the presence of a compound layer causes the appearance of a more abrasion-wear component as the compound layer breaks down during sliding and becomes hard [28].

Fig. 10 shows the SEM-EDS morphologies of the worn surfaces for sample 3 (Fig.10a,b) and sample 7 (Fig.10c,d) demonstrating the different wear mechanisms under both 5 N and 9 N loads. The EDS results show oxygen rich areas, which suggests oxidative wear on the modified surfaces. When load increases, the characterization of wear mechanism has changed and severe wear rate intensity is seen as in Fig. 10(b and d). The worn surfaces exhibited a seizure of the wear debris on the sliding surface and the subsequent abrasive deformation is evidenced by the micro-cracks on the surface. The nitrides phases on surface was affected to characterization of wear. The brittle layer was formed delamination zone [16]. Cracks, wear debris and surface layer delamination were observed at the modified surface. Parallel groves in the direction of the intended displacement were formed at the worn area [25–28,31].

Fig. 11(a and b) display the AFM results of the surface for sample 3 after wear test. The surface morphology is usually flat and compact; the structural defects include small holes or caves. The abrasive wear was formed on the surface. Surface ruptures formed during the wear test on the surface, and trenches formed due to material removal as well as wear debris near the 2000 nm × 20 nm area. The regions where higher asperities occurred were maintained by their high wear resistance. The wear depth is not high. The surface topography was well described even when the load increases [31,32].

The character of the surface layer after the wear test is clearly visible by AFM analysis. Fig. 12(a and b) show the specimen-5 also suffered from a combination of adhesive and abrasive wear with a smoother wear track was gained. The difference of elevation on surfaces can be seen easily, while the load changes. The height of yellow colour area is higher than that of red area. There is cleavage failure between modificated surface layers due to wear process.

4.   Conclusions

- The microstructure of the surface layer in all plasma-modified specimens consisted of a compound layer and a diffusion zone from the surface to inward.
- The rapid heating - cooling and diffusion leading to a decrease in grain size on the surface.
- The process parameters, such as the nozzle distance and the number of pulses, were necessary to improve and change the surface mechanical properties. The thickness of the modified layer increased with increasing number of pulses and at the optimum nozzle distance.
- The consumable electrode causes the ionization of Tungsten (W) and Nitrogen (N) atoms where and these ions are doped into the surface by means of diffusion mechanism.
- The surface modification process for the AISI 4140 steel produced a surface layer with more favorable properties. Tungsten and nitride-rich phases such as $Fe_{2\text{-}3}N$, W_3O, W, FeN and γ-Fe were formed; due to the pulse plasma treatment. The intensity of peak which stands for the relevant phases was increased with increased number of pulse
- The hardness value of 4140 steel can be increased up to 4–6 times higher compared to untreated sample in a very short time (e.g. 1 min.) by means of pulse plasma treatment. The new hard phases and structure were improved the microhardness value. The increase in pulse number of energy absorbed by the surface leads to the increase in microhardness value
- The modified layer provided wear and anti-scuffing properties to the surface. The wear resistance of the modified surface was approximately 2–3 times greater than unmodified surface due to the change in the modified surface. The hard phases and structure play a key role in improving the wear resistance by increasing the surface properties.
- The friction coefficients were decreased after the pulse plasma treatment.
- The values of wear resistance and friction coefficients are changed with process parameters.
- The process parameters affected the wear properties such as number of pulse and distance.
- When the increase the number of pulse increased, the wear rate was decreased.
- Wear rate and coefficient of friction were decreased while the nozzle distance decreased
- Abrasive and adhesive wear were occurred on surface. There were small cracks on surface after wear test.

Acknowledgment

Appendix A. Supplementary data

Supplementary material related to this article can be found, in the online version, at doi:https://doi.org/10.1016/j.jmrt.2019.12.048.

REFERENCES

[1] Byrkaa OV, Chebotareva VV, Derepovskia NT, Müllerb G, Schumacherb G, et al. Properties of modified surface layers of industrial steel samples processed by pulsed plasma streams. Vacuum 2000;58:195–201.

[2] Sartowskaa B, Piekoszewskia J, Waliśa L, Stanisławski J, Nowicki L, Ratajczak R, et al. Thermal stability of the phases formed in the near surface layers of unalloyed steels by nitrogen pulsed plasma treatment. Vacuum 2007;81:1188–90.

[3] Podgornik B, Vižintin J. Sliding and pitting wear resistance of plasma and pulse plasma nitrided steel. Surf Eng 2001;17(4):300–4.

[4] Özbek YY, Durman M, Akbulut H. Wear behaviour of steel modıfıed by pulse plasma technıque. Tribol Trans 2009;52:213–22.

[5] Bolton M, Cockrem J, Farinotti A. Pulse plasma nitriding for plasma vapour deposition coating of high speed steels. Surf Eng 2004;20(3):167–73.

[6] Uglov VV, Anishchik VM, Cherenda NN, Sveshnikov YuV, Astashynski VM, Kostyukevich EA, et al. The formation of a tungsten containing surface layer in a carbon steel by compression plasma flow. Surf Coat Technol 2008;202:2439–42.

[7] Podgornik B, Hogmark S, Sandberg O, Leskovsek V. Wear resistance and anti-sticking properties of duplex treated forming tool steel. Wear 2003;254:1113–21.

[8] Tyurin NY, Kolısnıchenko OV, Tsygankov NG. The pulse plasma technology. Paton Weld J 2004;1:38–43.

[9] Langnera J, Piekoszewskia J, Wernera Z, Tereshin VI, Chebotarev VV, Garkusha I, et al. Surface modification of constructional steels by irradiation with high intensity pulsed nitrogen plasma beams. Surf Coat Technol 2000;128-129:105–11.

[10] Ulutan M, Celik ON, Gasan H, Er U. Effect of different surface treatment methods on the friction, wear behavior of AISI 4140 steel. J Mater Sci Technol 2010;26:251–7.

[11] Dewana MW, Lianga J, Wahaba MA, Oke AM. Effect of post-weld heat treatment and electrolytic plasma processing on tungsten inert gas welded AISI 4140 alloy steel. Mater Des 2014;54:6–13.

[12] Sartowska B, Piekoszewski J, Wali L, Kopcewicz M, Werner Z, Stanislawski J, et al. Phase changes in steels irradiated with intense pulsed plasma beams. Vacuum 2003;70:285–91.

[13] Li CX, Sun b Y, Bell T. Factors influencing fretting fatigue properties of plasma-nitrided low alloy steel. Mater Sci Eng 2000;A292:18–259.

[14] Sirin SY, Sirin K, Kaluc E. Effect of the ion nitriding surface hardening process on fatigue behavior of AISI 4340 steel. Mater Charact 2008;59:351–8.

[15] Ozbek YY, Sarioglu C, Durman M. The effect of plasma detonation parameters on residual stresses developed in the plasma modified layer. Vacuum 2014;106:11–5.

[16] Guana QF, Zoua H, Zoua GT, Wub AM, Haob SZ, Zoub JX, et al. Surface nanostructure and amorphous state of a low carbon steel induced by high-current pulsed electron beam. Surf Coat Technol 2005;196:145–9.

[17] Anishchika VM, Uglova VV, Astashynskia VV, Astashynski VM, Ananinb SI, Kostyukevichb EA, et al. Compressive plasma flows interaction with steel surface: structure and mechanical properties of modified layer. Vacuum 2003;70:269–74.

[18] Amanov A, Sik Pyun Y, Sasaki S. Effects of ultrasonic nanocrystalline surface modification (UNSM) technique on the tribological behavior of sintered Cu-based alloy. Tribol Int 2014;72:187–97.

[19] Yana MF, Wua YQ, Li RL. Grain and grain boundary characters in surface layer of untreated and plasma nitrocarburized 18Ni maraging steel with nanocrystalline structure. Appl Surf Sci 2013;273:520–6.

[20] Özbek YY, Akbulut H, Durman M. Surface properties of M2 steel treated by pulse plasma technique. Vacuum 2015;122:90–5.

[21] Gualtieri E, Borghi A, Calabri L, Pugno N, Valeri S. Increasing nanohardness and reducing friction of nitride steel by laser surface texturing. Tribol Int 2009;42:699–705.

[22] Wang YX, Yan MF, Li B, Guo LX, Zhang CS, Zhang YX, et al. Surface properties of low alloy steel treated by plasma nitrocarburizing prior to laser quenching process. Opt Laser Technol 2015;67:57–64.

[23] Sartowska B, Piekoszewski J, Waliś L, Senatorski J, Stanisławski J, Ratajczak R, et al. Structural and tribological properties of carbon steels modified by plasma pulses containing inert and active ions. Surf Coat Technol 2007;201:8295–8.

[24] Dingshun S, Wen Y, Zhiqiang F, Yanhong G, Chengbiao W, Jiajun L. The effect of nitriding temperature on hardness and microstructure of die steel pre-treated by ultrasonic cold forging technology. Mater Des 2013;49:392–9.

[25] Zhanga CS, Yana MF, Suna Z, Wanga YX, Youa Y, Baib B, et al. Optimizing the mechanical properties of M50NiL steel by plasmanitrocarburizing. Appl Surf Sci 2014;315:28–35.

[26] Yanqiu X, Shijie W, Feng Z, Haizhong W, Yimin L, Tao X. Tribological properties of plasma nitrided stainless steel against SAE52100 steel under ionic liquid lubrication condition. Tribol Int 2006;39:635–40.

[27] Yang L, Liang W, Dandan Z, Shen Lie. The effect of surface nanocrystallization on plasma nitriding behaviour of AISI 4140 steel. Appl Surf Sci 2010;257:979–84.

[28] Fattah M, Mahboubi F. Comparison of ferritic and austenitic plasma nitriding and nitrocarburizing behavior of AISI 4140 low alloy steel. Mater Des 2010:3915–21.

[29] Yan MF, Wanga YX, Chen XT, Guo LX, Zhang CS, You Y, et al. Laser quenching of plasma nitrided 30CrMnSiA steel. Mater Des 2014;58:154–60.

[30] Gangopadhyay S, Acharya R, Chattopadhyay AK, Paul S. Effect of substrate bias voltage on structural and mechanical properties of pulsed DC magnetron sputtered TiN–MoSx composite coatings. Vacuum 2010;84:843–50.

[31] Shaha MS, Saleema M, Ahmada R, Zakaullah M, Qayyuma A, Murtaza G. Langmuir probe, characterization of nitrogen plasma for journal of materials processing technology surface nitriding of AISI-4140 steel. J Mater Process Technol 2008;199:363–8.

[32] Jradi K, Schmitt M, Bistac S. Influence of the surface chemistry on the nanotribological behaviour of (AFM tip/graphite) couples. Appl Surf Sci 2012;258:4687–97.